

# Solar Oscillations and Convection: I. Formalism for Radial Oscillations

Å. Nordlund

*Theoretical Astrophysics Center, and Astronomical Observatory,  
Juliane Maries Vej 30, 2100 Copenhagen Ø, Denmark*

[aake@astro.ku.dk](mailto:aake@astro.ku.dk)

and

R. F. Stein

*Dept. of Physics and Astronomy, Michigan State University, East Lansing, MI 48823, U.S.A.  
[bob@steinr.pa.msu.edu](mailto:bob@steinr.pa.msu.edu)*

## ABSTRACT

We present a formalism for investigating the interaction between p-mode oscillations and convection by analyzing realistic, three-dimensional simulations of the near-surface layers of the solar convection zone. By choosing suitable definitions for fluctuations and averages, we obtain a separation that retains exact equations. The equations for the horizontal averages contain one part that corresponds directly to the wave equations for a 1-D medium, plus additional terms that arise from the averaging and correspond to the turbulent pressure gradient in the momentum equation and the divergence of the convective and kinetic energy fluxes in the internal energy equation. These terms cannot be evaluated in closed form, but they may be measured in numerical simulations. The additional terms may cause the mode frequencies to shift, relative to what would be obtained if only the terms corresponding to a 1-D medium were retained—most straightforwardly by changing the mean stratification, and more subtly by changing the effective compressibility of the medium. In the presence of time dependent convection, the additional terms also have a stochastic time dependence, that acts as a source of random excitation of the coherent modes. In the present paper, we derive an expression for the excitation power and test it by applying it to a numerical experiment of sufficient duration for the excited modes to be spectrally resolved.

*Subject headings:* sun:oscillations- sun:p-modes- sun:convection- sun:numerical simulation

## 1. Introduction

The near-surface layers of the Sun are of crucial importance for the properties of the solar p-mode oscillations (see the recent conference proceedings; Brown 1993; Hoeksema et al. 1995; Ulrich et al. 1995; Antia & Chitre 1996; Pijpers et al. 1997). The upper turning points of the p-modes are located in these layers and this is where the modes are excited and damped. This is also where the solar convection zone gives way to the visible solar

photosphere.

The thin superadiabatic layer at the top of the solar convection zone is characterized by large fluctuations in the thermodynamic variables. As illustrated by detailed numerical simulations of the solar surface layers (Nordlund 1982, 1985; Steffen et al. 1989; Nordlund & Dravins 1990; Nordlund & Stein 1991a; Steffen & Freytag 1991; Stein & Nordlund 1989, 1991, 1994, 1998; Atroschenko & Gadun 1994; Solanki et al. 1996), the fluctuation amplitudes peak just below the visible surface,

where the temperature ranges from 5000 to 10,500 K, and the logarithmic fluctuations of the density and pressure,  $\Delta \ln \rho$  and  $\Delta \ln P$ , are of the order of unity. The velocity amplitudes are large throughout the photosphere, with rms Mach numbers of the order of 0.3 and peak Mach numbers exceeding unity in a small fraction of the volume (Nordlund & Stein 1991b; Stein & Nordlund 1998).

The layers with large amplitude fluctuations (at recent meetings referred to as the ‘muck region’) may be expected to influence the solar p-mode oscillations in several ways. First, these are the layers where most of the random excitation of modes is expected to occur (Stein 1967, 1968; Goldreich & Keeley 1977; Goldreich & Kumar 1988, 1990; Stein & Nordlund 1991; Bogdan et al. 1993; Goldreich et al. 1994; Musielak et al. 1994). Second, the average vertical stratification of this region cannot be assumed to be in hydrostatic equilibrium; the motions will contribute an additional ‘turbulent pressure’, that adds to the normal gas pressure and hence tends to elevate the surface layers. The large amplitude, non-linear fluctuations makes even the definition of appropriate average values a non-trivial exercise. Further, due to the extreme temperature sensitivity of the opacity in the surface layers the emergent solar luminosity is produced by an average state that differs noticeably from that of a corresponding one dimensional model. Third, because of the presence of the fluctuations, the wave propagation properties of the medium will in general be different than for a homogeneous medium. We follow Balmforth (1992a) and refer to the effects due to mean structure changes as ‘extrinsic’ (or ‘model’) effects, and those that are caused by changes in the wave propagation properties of the medium as ‘intrinsic’ (‘modal’ or ‘mode physics’) effects.

A problem with reproducing the frequencies of the modes that have upper turning points in these layers has indeed been known since the early days of helioseismology (Christensen-Dalsgaard et al. 1996b; Christensen-Dalsgaard 1988; Christensen-Dalsgaard et al. 1988). Improvements in the calculation of the equation of state (Mihalas et al. 1990; Rogers et al. 1996) did not improve the situation, but instead rather sharpened the significance of the discrepancy between the observed and calculated oscillation frequencies.

The discrepancy between the observed and the-

oretical mode frequencies is primarily a function of frequency and is nearly independent of degree,  $\ell$ , for small  $\ell$ . It is small for the lowest frequencies, and grows to significant values for frequencies approaching the cut-off frequency of the solar photosphere (approximately 5 mHz). This shows that the cause of the discrepancy resides in layers to which the low frequency modes hardly penetrate, but where the high frequency modes have a significant amplitude. Thus, the source of the discrepancy must lie near the solar surface, in the outer layers of the solar cavity.

Stochastic excitation of p-modes has been demonstrated in numerical simulations of convection in the solar surface layers (Stein et al. 1988; Steffen 1988; Stein et al. 1989; Stein & Nordlund 1991; Bogdan et al. 1993). In principle, the various contributions to stochastic excitation, damping and frequency shift may be directly measured in such numerical simulations. Alternatively, one may instead extract information about the model structure and mode propagation properties from the numerical simulations, and carry that information over to standard envelope and mode calculation procedures. The advantage with the latter method is that one is not limited to the studying the sparse spectrum of modes that are excited in a small box. The main purpose of the present paper is to present a formalism for interpreting quantities used in such 1-D calculations as suitable averages of quantities that may be measured in 3-D numerical simulations.

Stein & Nordlund (1991) used a simplified version of the formalism presented here in an initial study of mode excitation and Rosenthal et al. (1999); Rosenthal et al. (1998) also used a simplified version to analyze the effect of 1-D/3-D model differences on the frequencies of radial modes, showing that on the one hand the model differences may account for the majority of the frequency discrepancy, but that on the other hand the modal effects also are significant.

In the present paper we develop a formalism for analyzing the interaction of convection with purely radial oscillations by choosing an exact decomposition into horizontal averages and fluctuations. Since most p-modes are nearly radial near the solar surface, the analysis covers the lower order behavior of non-radial modes as well.

In Section 2 we present the separation of vari-

ables that we have chosen to work with. In Section 3 we use this formalism to analyze how the interaction of convection with the oscillations can cause mode excitation, mode damping and frequency shifts, and in Section 4 we show by explicit application to a numerical experiment that the expression for the mode excitation produces estimates of mode power that are consistent with what is actually observed in the experiment.

In order to verify the formula for the mode excitation it is necessary to use a numerical experiment of sufficiently long duration for the excited modes to be spectrally resolved, because this allows the mode excitation power to be estimated directly from a measurement of the mode power and the mode lifetime (obtainable from the full-width-at-half-maximum of the mode energy). This necessitates a relatively low spatial resolution, which precludes a direct comparison with the solar mode excitation power (currently well established, see for example Roca Cortes et al. (1999)).

In a subsequent paper (Paper II) we make use of simulations with higher spatial resolution (and correspondingly shorter duration), that allow us to make detailed comparisons with helioseismic data, and to explore details of the processes that dominate the stochastic mode excitation.

## 2. Formalism

Ideally, we would like to split the fluid equations into one set describing the oscillations and one set describing convection. By the very nature of the problem, such a separation cannot be complete; if the convection is to excite the oscillations, it must give rise to a source term in what would otherwise be equations describing ideal, radial wave motions. And if convection is to have an effect on the (complex) frequencies of the modes, there must be a possibility for convection to affect the compressibility of the gas; in other words to have a coherent response with a phase lag that in general may be expected to vary with height. In addition, the convection is able to affect the frequencies in a more trivial manner, namely by changing the overall stratification relative to whatever reference 1-D model one happens to compare with.

We are thus content with, and indeed looking for, a separation consisting of wave-like equations with additional terms that are related to the pres-

ence of convection. Such a separation is possibly not unique, but below we present one possibility.

One factor influencing our choice of separation was that we are here concerned with a case that is, in a sense, opposite to the more common case of small amplitude 3-D fluctuations on top of large means. We have large amplitude 3-D fluctuations due to convection on top of a mean with small amplitude coherent p-mode fluctuations. Thus we prefer to work with the actual equations, rather than some truncated expansion. We retain explicitly those terms that cannot be worked out analytically, and subsequently measure them in the numerical simulations. In doing so, we wish to make the split such that these terms have a well defined physical meaning, and are numerically well conditioned.

### 2.1. Notation and definitions

To achieve the goals set out above, it is crucial to choose an appropriate set of definitions for fluctuations and averages. We use the convention that per-unit-volume quantities are written in upper case and per-unit-mass quantities are written in lower case.

For the present case of purely radial motions, we define straight horizontal averages  $\bar{F}$  and corresponding residuals  $\check{F}$  for per-unit-volume variables  $F$ ,

$$\bar{F}(z, t) = \langle F \rangle_{xy} \quad (1)$$

$$\check{F}(x, y, z, t) = F(x, y, z, t) - \bar{F}(z, t), \quad (2)$$

and density weighted horizontal averages  $\bar{f}$  with residuals  $\check{f}$  for per-unit-mass variables  $f$ ,

$$\bar{f}(z, t) = \langle \rho f \rangle_{xy} / \langle \rho \rangle_{xy} \quad (3)$$

$$\check{f}(x, y, z, t) = f(x, y, z, t) - \bar{f}(z, t). \quad (4)$$

Thus, horizontal averages vanish for residuals of per-unit-volume variables,

$$\langle \check{F} \rangle_{xy} = 0, \quad (5)$$

while for the residuals of per-unit-mass variables it is the *mass weighted* horizontal averages

$$\langle \rho \check{f} \rangle_{xy} = 0 \quad (6)$$

that vanish.

Because of the large number of occurrences of horizontal averages, we henceforth drop their explicit  $xy$  subscript ( $\langle \rangle_{xy} \rightarrow \langle \rangle$ ) and retain subscripts only on time averages ( $\langle \rangle_t$ ) and ensemble averages ( $\langle \rangle_{\text{ens}}$ ).

As a consequence of Eq. 3, products of two and three per-unit-mass variables obey

$$\langle \rho f g \rangle = \langle \rho \check{f} \check{g} \rangle + \bar{\rho} \bar{f} \bar{g} \quad (7)$$

$$\begin{aligned} \langle \rho f g h \rangle &= \langle \rho \check{f} \check{g} \check{h} \rangle + \bar{\rho} \bar{f} \bar{g} \bar{h} + \\ &\quad \langle \rho \check{g} \check{h} \rangle \bar{f} + \langle \rho \check{f} \check{h} \rangle \bar{g} + \langle \rho \check{f} \check{g} \rangle \bar{h} \end{aligned} \quad (8)$$

## 2.2. 1-D averaged equations

To derive a set of hydrodynamic equations for the horizontal averages, we apply the formalism of the previous subsection to the three-dimensional equations of mass, momentum and energy conservation,

$$\frac{\partial}{\partial t}(\rho) = -\nabla \cdot (\rho \mathbf{u}), \quad (9)$$

$$\frac{\partial}{\partial t}(\rho \mathbf{u}) = -\nabla \cdot (\rho \mathbf{u} \mathbf{u} - \sigma) - \nabla P - \rho \mathbf{g}, \quad (10)$$

$$\begin{aligned} \frac{\partial}{\partial t}(\rho e_i) &= -\nabla \cdot (\rho e_i \mathbf{u}) - P(\nabla \cdot \mathbf{u}) \\ &\quad - \nabla \cdot \mathbf{F}_{\text{rad}} + Q_{\text{diss}}, \end{aligned} \quad (11)$$

where  $e_i$  is the internal energy,  $P = P(\rho, e_i)$  is the gas pressure, and  $\mathbf{F}_{\text{rad}}$  is the radiative energy flux.  $Q_{\text{diss}}$  is the viscous dissipation

$$Q_{\text{diss}} = \sum_{ij} \sigma_{ij} s_{ij}, \quad (12)$$

where  $s_{ij}$  is the symmetric part of the strain tensor  $\partial u_i / \partial x_j$ , and  $\sigma_{ij}$  is the viscous stress tensor,  $\sigma_{ij} = \rho \nu s_{ij}$ .

By Eqs. 7–8, the total kinetic energy  $\langle \frac{1}{2} \rho u^2 \rangle$  splits into the kinetic energy of the radial motion and of the horizontal fluctuations,

$$\langle \frac{1}{2} \rho u^2 \rangle = \frac{1}{2} \bar{\rho} \bar{u}_z^2 + \langle \frac{1}{2} \rho \check{u}^2 \rangle, \quad (13)$$

and the radial kinetic energy flux  $\langle \frac{1}{2} \rho u^2 \bar{u}_z \rangle$  splits into

$$\begin{aligned} \langle \frac{1}{2} \rho u^2 \bar{u}_z \rangle &= \frac{1}{2} \bar{\rho} \bar{u}_z^2 \bar{u}_z + \langle \frac{1}{2} \rho \check{u}^2 \rangle \bar{u}_z \\ &\quad + \langle \rho \check{u}_z^2 \rangle \bar{u}_z + \langle \frac{1}{2} \rho \check{u}^2 \check{u}_z \rangle. \end{aligned} \quad (14)$$

The terms on the RHS may be interpreted as the kinetic energy flux of the radial motions, the advection of convective kinetic energy density by the radial motions, the  $Pu$  flux associated with the turbulent pressure (cf. below), and the radial kinetic energy flux associated with the horizontal fluctuations.

An equation for conservation of total internal plus kinetic energy,  $e = e_i + e_k$ , may be obtained by adding the time derivative of the kinetic energy density,  $e_k = \frac{1}{2} u^2$ , to that for the internal energy  $e_i$ ,

$$\frac{\partial}{\partial t}(\rho e) = -\nabla \cdot (\rho e \mathbf{u} + P \mathbf{u} + \mathbf{F}_{\text{rad}} + \mathbf{F}_{\text{visc}}) + \rho \mathbf{u} \cdot \mathbf{g}, \quad (15)$$

where  $\mathbf{F}_{\text{visc}}$  is the viscous flux

$$F_{\text{visc},i} = -\sum_j u_j \sigma_{ij}. \quad (16)$$

Horizontal averaging of the above equations yields equations that depend on height and time, but not on the horizontal coordinates:

$$\frac{\partial}{\partial t}(\bar{\rho}) = -\frac{\partial}{\partial z}(\bar{\rho} \bar{u}_z), \quad (17)$$

$$\begin{aligned} \frac{\partial}{\partial t}(\bar{\rho} \bar{u}_z) &= -\frac{\partial}{\partial z}(\bar{\rho} \bar{u}_z^2 + \bar{P}_g - \bar{\sigma}_{zz}) + g \bar{\rho} \\ &\quad \left[ -\frac{\partial}{\partial z}(\bar{P}_t) \right], \end{aligned} \quad (18)$$

$$\begin{aligned} \frac{\partial}{\partial t}(\bar{\rho} \bar{e}_i) &= -\frac{\partial}{\partial z}(\bar{\rho} \bar{e}_i \bar{u}_z) - \bar{P}_g \frac{\partial \bar{u}_z}{\partial z} \\ &\quad \left[ -\frac{\partial}{\partial z}(\bar{F}_{\text{conv}} + \bar{F}_{\text{rad}}) \right. \\ &\quad \left. + Q_{\text{diss}} + \langle \check{\mathbf{u}} \cdot \nabla P \rangle \right], \end{aligned} \quad (19)$$

$$\begin{aligned} \frac{\partial}{\partial t}(\bar{\rho} \bar{e}) &= -\frac{\partial}{\partial z}(\bar{\rho} \bar{e} \bar{u}_z + \bar{P} \bar{u}_z) + g \bar{\rho} \bar{u}_z \\ &\quad \left[ -\frac{\partial}{\partial z}(\bar{F}_{\text{conv}} + \bar{F}_{\text{rad}}) \right. \\ &\quad \left. + \bar{F}_{\text{kin}} + \bar{F}_{\text{visc}} \right], \end{aligned} \quad (20)$$

where  $\bar{\rho} = \langle \rho \rangle$ ,  $\bar{\rho} \bar{u}_z = \langle \rho u_z \rangle$ ,  $\bar{P}_g = \langle P_g \rangle$ ,  $\bar{P} = \bar{P}_g + \bar{P}_t$ , and  $\bar{\rho} \bar{e} = \langle \rho e \rangle$ .  $\bar{P}_t$  and  $\bar{F}_{\text{conv}}$  are defined below (Eqs. 21–22).

Equations 17–20 correspond closely to the hydrodynamic equations for a stratified, homogeneous 1-D medium. The terms that are not bracketed are exactly what appear in the 1-D equations,

whereas the extra, bracketed terms are due to the convective motions. These are the gradient of the turbulent pressure

$$\bar{P}_t = \langle \rho \ddot{u}_z^2 \rangle, \quad (21)$$

the divergence of the convective flux

$$\bar{F}_{\text{conv}} = \langle (\rho e_i + P_g) \ddot{u}_z \rangle, \quad (22)$$

and the divergence of the kinetic energy flux associated with convection,

$$\bar{F}_{\text{kin}} = \langle (\frac{1}{2} \rho u^2) \ddot{u}_z \rangle. \quad (23)$$

Here  $\ddot{u}_z$  is the vertical velocity relative to a frame of reference moving with velocity  $\bar{u}_z = \langle u_z \rho \rangle / \langle \rho \rangle$ ; we refer to this frame of reference as ‘pseudo-lagrangian’. Note that, in general,  $\langle \ddot{u}_z \rangle \neq 0$ .

The  $\bar{F}_{\text{rad}}$  term should, in principle, not be bracketed, since it also may appear in a 1-D medium. It is, however, so intimately related to the other flux terms that we prefer to place it inside the brackets. Furthermore, because of the strong non-linearities involved, the value of  $\bar{F}_{\text{rad}}$  may differ substantially between 1-D and 3-D models with the same average structure.

A stationary state that has  $\bar{u}_z = 0$  obeys

$$\frac{\partial}{\partial z} (\bar{P}_g + \bar{P}_t - \bar{\sigma}_{zz}) = g \bar{\rho} \quad (24)$$

$$\frac{\partial}{\partial z} (\bar{F}_{\text{conv}} + \bar{F}_{\text{kin}} + \bar{F}_{\text{visc}} + \bar{F}_{\text{rad}}) = 0 \quad (25)$$

Note that the horizontally averaged pressure is in general not the same as the pressure for the average density and energy of which it is a function. Because of the correlation of the fluctuations and the contribution from higher order terms,

$$\bar{P}_g = P_g(\bar{\rho}, \bar{e}) + \frac{\partial^2 P_g}{\partial \rho \partial e} \langle \bar{\rho} \bar{e} \rangle + \text{higher order terms} \quad (26)$$

is in general not equal to  $P_g(\bar{\rho}, \bar{e})$ .

### 2.3. Pseudo-Lagrangian 1-D Equations

For the purpose of studying adiabatic (or near adiabatic) wave mode fluctuations, it is more relevant to write the horizontally averaged equations in the pseudo-lagrangian reference frame (moving with velocity  $\bar{u}_z$ ). The operator

$$\frac{D}{Dt}() = \frac{\partial}{\partial t}() + \bar{u}_z \frac{\partial}{\partial z}(), \quad (27)$$

picks up the time variation in that frame of reference. For a per-unit-mass variable  $f$  that satisfies

$$\frac{\partial}{\partial t}(\rho f) = -\nabla \cdot F, \quad (28)$$

the change to a pseudo-lagrangian frame results in

$$\begin{aligned} \frac{D}{Dt}(\rho f) &= -\nabla \cdot F + \bar{u}_z \frac{\partial}{\partial z}(\rho f) \\ &= -\nabla \cdot (F - \rho f \bar{\mathbf{u}}) - \rho f \frac{\partial}{\partial z}(\bar{u}_z), \end{aligned} \quad (29)$$

i.e., the subtraction of the average flux of  $\rho f$  from within the divergence operator, and the addition of a term of the form  $-\rho f \frac{\partial}{\partial z}(\bar{u}_z)$ , that accounts for the dilation or concentration of the (per unit volume) quantity  $\rho f$ , corresponding to stretching or compression of the coordinate system.

In terms of the  $\frac{D}{Dt}()$  operator the averaged 1-D equations become

$$\frac{D}{Dt}(\bar{\rho}) = -\bar{\rho} \frac{\partial}{\partial z}(\bar{u}_z) \quad (30)$$

$$\begin{aligned} \frac{D}{Dt}(\bar{\rho} \bar{u}_z) &= -\frac{\partial}{\partial z}(\bar{P}_g - \bar{\sigma}_{zz}) + g \bar{\rho} - \bar{\rho} \bar{u}_z \frac{\partial}{\partial z}(\bar{u}_z) \\ &\quad [-\frac{\partial}{\partial z}(\bar{P}_t)], \end{aligned} \quad (31)$$

$$\begin{aligned} \frac{D}{Dt}(\bar{\rho} \bar{e}) &= -\frac{\partial}{\partial z}(\bar{P} \bar{u}_z) + g \bar{\rho} \bar{u}_z - \bar{\rho} \bar{e} \frac{\partial}{\partial z}(\bar{u}_z) \\ &\quad [-\frac{\partial}{\partial z}(\bar{F}_{\text{conv}} + \bar{F}_{\text{kin}} + \bar{F}_{\text{visc}} + \bar{F}_{\text{rad}})]. \end{aligned} \quad (32)$$

The transformation between per-unit-volume and per-unit-mass pseudo-lagrangian time derivatives is

$$\begin{aligned} \bar{\rho} \frac{D}{Dt}(\bar{f}) &= \frac{D}{Dt}(\bar{\rho} \bar{f}) - \bar{f} \frac{D}{Dt}(\bar{\rho}) \\ &= \frac{D}{Dt}(\bar{\rho} \bar{f}) + \bar{\rho} \bar{f} \frac{\partial}{\partial z}(\bar{u}_z). \end{aligned} \quad (33)$$

The dilation term that is present in the per-unit-volume formulation thus drops out in the per-unit-mass formulation, because a fixed amount of mass is under consideration—the mass element  $\bar{\rho} dz$  is indeed suitable for depth integration of pseudo-lagrangian per-unit-mass quantities.

In per-unit-mass variables, the equation of motion and the energy equations for horizontal averages thus become

$$\bar{\rho} \frac{D}{Dt}(\bar{u}_z) = -\frac{\partial}{\partial z}(\bar{P}_g + \bar{P}_t - \bar{\sigma}_{zz}) + g \bar{\rho}, \quad (34)$$

$$\begin{aligned} \bar{\rho} \frac{D}{Dt}(\bar{e}_i) &= -\bar{P}_g \frac{\partial \bar{u}_z}{\partial z} \\ &[ -\frac{\partial}{\partial z}(\bar{F}_{\text{conv}} + \bar{F}_{\text{rad}}) \\ &+ Q_{\text{diss}} + \langle \bar{\mathbf{u}} \cdot \nabla P \rangle], \end{aligned} \quad (35)$$

$$\begin{aligned} \bar{\rho} \frac{D}{Dt}(\bar{e}) &= -\frac{\partial}{\partial z}(\bar{P} \bar{u}_z) + g \bar{\rho} \bar{u}_z \\ &[ -\frac{\partial}{\partial z}(\bar{F}_{\text{conv}} + \bar{F}_{\text{rad}}) \\ &+ \bar{F}_{\text{kin}} + \bar{F}_{\text{visc}}]. \end{aligned} \quad (36)$$

In what follows, we use the traditional notation  $\delta \bar{P}_g$ ,  $\delta \bar{\rho}$ , etc., to distinguish pseudo-lagrangian perturbations from Eulerian ones.

### 3. Interactions between oscillations and convection

We now use this formalism to calculate the work done on radial oscillation modes by convection. We then test the resulting expression on the vertical resonant modes excited in a numerical simulation of solar convection.

In the presence of a coherent mode, the time variation of the additional, convective terms in Eqs. 17–20 is partly in unison with the mode, reflecting the coherent response of convection to the presence of the mode. The coherent response may again be divided into one part that is in phase with the mode (appearing as the real part of a Fourier transform), and one part that is in quadrature with the mode (the imaginary part of a Fourier transform). The imaginary part of the coherent component causes an exponential damping (or growth) of a trapped mode, and the real part causes a frequency shift. In analogy with simpler situations we also refer to these parts as “adiabatic” and “non-adiabatic”. There is also an incoherent contribution, corresponding to the random variation of the convection, that contributes to these averages, and produces stochastic mode excitation and damping.

The equation describing the time evolution of the mode kinetic energy may be obtained from Eq. 34:

$$\begin{aligned} \bar{\rho} \frac{D}{Dt} \left( \frac{1}{2} \bar{u}_z^2 \right) &= -\frac{\partial}{\partial z} [\bar{u}_z (\bar{P}_g + \bar{P}_t - \bar{\sigma}_{zz})] \\ &+ (\bar{P}_g + \bar{P}_t - \bar{\sigma}_{zz}) \frac{\partial \bar{u}_z}{\partial z} \\ &+ \bar{\rho} \bar{u}_z g. \end{aligned} \quad (37)$$

Integrating over time and depth, we obtain

$$\begin{aligned} \left[ \int dM \frac{1}{2} \bar{u}_z^2 \right]_0^t &= \int dt \int dz (\delta \bar{P}_g + \delta \bar{P}_t \\ &- \delta \bar{\sigma}_{zz}) \frac{\partial \bar{u}_z}{\partial z} \\ &+ \int dt \int dz \bar{\rho} \bar{u}_z g \\ &+ [\dots]_{\text{boundaries}}. \end{aligned} \quad (38)$$

where,  $[\dots]_{\text{boundaries}}$  denotes the boundary contributions that result from integrating the divergence form of the equation. For suitably chosen boundary conditions, these contributions vanish. Specifically, the displacement may be chosen to vanish at the lower boundary, and the pressure may be chosen sufficiently small at the upper boundary. The work done by gravity vanishes if there are no net mass displacements in the model.

The  $\int dt \int dz (\delta \bar{P}_g + \delta \bar{P}_t - \delta \bar{\sigma}_{zz}) \partial \bar{u}_z / \partial z$  part of the work integral represents the PdV work done by the gas pressure, the turbulent pressure, and the mean viscous stress. (The mean viscous stress may be expected to be negligibly small in stellar atmospheres and envelopes, and should be small also in numerical simulations.) The  $\partial \bar{u}_z / \partial z$  factor is equal to  $-D \ln \bar{\rho} / Dt = D \ln V / Dt$ , where  $V$  is the specific volume. Pressure perturbations must be out of phase with density perturbations in order to contribute to the work integral. In a diagram showing  $\delta \bar{P}$  against  $\delta \bar{\rho}$  this corresponds to open curves, with a counter clockwise sense of orientation.

The signs are as to be expected from basic physical principles; the mode kinetic energy increases if the pressure is larger during expansion than during compression.

#### 3.1. Coherent and incoherent fluctuations

The PdV work integral, Eq. 38, is

$$W = \int dt \int dz \delta \bar{P} \frac{\partial \dot{\xi}}{\partial z}. \quad (39)$$

Here  $\delta \bar{P}$  is the pseudo-lagrangian total pressure fluctuation (neglecting the small viscous stress contribution)

$$\delta \bar{P} = \delta \bar{P}_g + \delta \bar{P}_t, \quad (40)$$

and  $\xi$  is the displacement, which is related to the velocity by

$$\xi = \int^t dt' \bar{u}_z, \quad (41)$$

and to the density variations by

$$\frac{D \ln \bar{\rho}}{Dt} = -\frac{\partial \dot{\xi}}{\partial z}. \quad (42)$$

The displacement and the pressure fluctuations can be split into two parts: one the coherent, sinusoidal, modal part and the other the incoherent, random part:

$$\xi = \xi_\omega + \xi_r \quad (43)$$

$$\delta \bar{P} = \delta \bar{P}_\omega + \delta \bar{P}_r. \quad (44)$$

The pressure fluctuations can be further split into an adiabatic part, proportional to the density fluctuations,

$$\delta \ln \bar{P}^a = \Gamma_1(z) \delta \ln \bar{\rho} = -\Gamma_1(z) \frac{\partial \xi}{\partial z}, \quad (45)$$

and a non-adiabatic part, the remainder:

$$\delta \bar{P}_\omega = -\bar{P} \Gamma_1(z) \frac{\partial \xi_\omega}{\partial z} + \delta \bar{P}_\omega^n, \quad (46)$$

$$\delta \bar{P}_r = -\bar{P} \Gamma_1(z) \frac{\partial \xi_r}{\partial z} + \delta \bar{P}_r^n, \quad (47)$$

so that,

$$\delta \bar{P} = \delta \bar{P}_\omega^a + \delta \bar{P}_\omega^n + \delta \bar{P}_r^a + \delta \bar{P}_r^n. \quad (48)$$

Thus, the work integral can be expanded into the product of 4 pressure fluctuation terms multiplied by 2 displacement terms,

$$\begin{aligned} W &= \int \int dt dz \\ &[ \delta \bar{P}_\omega^a + \delta \bar{P}_\omega^n + \delta \bar{P}_r^a + \delta \bar{P}_r^n ] \left[ \frac{\partial \dot{\xi}_\omega}{\partial z} + \frac{\partial \dot{\xi}_r}{\partial z} \right] \\ &= \int \int dt dz \\ &[ (a) + (b) + (c) + (d) ] [ (1) + (2) ]. \quad (49) \end{aligned}$$

Consider the contribution of each possible pair to the work. The integral as a whole may be expected to display a “random walk” behavior; i.e., its expectation value grows with total time of integration. Contributions that are bounded are therefore

negligible. The  $(a) \times (1)$  contribution, for example,

$$(a) \times (1) \propto \frac{\partial \xi_\omega}{\partial z} \frac{\partial \dot{\xi}_\omega}{\partial z} \quad (50)$$

$$= \frac{D}{Dt} \left[ \frac{1}{2} \left( \frac{\partial \xi_\omega}{\partial z} \right)^2 \right] \quad (51)$$

$$\rightarrow \frac{1}{2} \left[ \left( \frac{\partial \xi_\omega}{\partial z} \right)^2 \right]_{t1}^{t2}, \quad (52)$$

is a total integral, so it is negligible.

$$(c) \times (2) \propto \frac{\partial \xi_r}{\partial z} \frac{\partial \dot{\xi}_r}{\partial z} \quad (53)$$

$$= \frac{D}{Dt} \left[ \frac{1}{2} \left( \frac{\partial \xi_r}{\partial z} \right)^2 \right] \quad (54)$$

$$\rightarrow \frac{1}{2} \left[ \left( \frac{\partial \xi_r}{\partial z} \right)^2 \right]_{t1}^{t2}, \quad (55)$$

so its contribution is also negligible.

$$(a) \times (2) + (c) \times (1) \propto$$

$$\bar{P} \Gamma_1 \frac{\partial \xi_\omega}{\partial z} \frac{\partial \dot{\xi}_r}{\partial z} + \bar{P} \Gamma_1 \frac{\partial \xi_r}{\partial z} \frac{\partial \dot{\xi}_\omega}{\partial z} =$$

$$\bar{P} \Gamma_1 \frac{D}{Dt} \left( \frac{\partial \xi_\omega}{\partial z} \frac{\partial \xi_r}{\partial z} \right)$$

$$\rightarrow \bar{P} \Gamma_1 \left[ \frac{\partial \xi_\omega}{\partial z} \frac{\partial \xi_r}{\partial z} \right]_{t1}^{t2}, \quad (56)$$

and also gives a negligible contribution. Note that this step depends on using the same  $\Gamma_1$  in the definitions of the adiabatic modal and random parts of the pressure fluctuation (Eqs. 46 and 47).

$$(b) \times (1) \propto \delta \bar{P}_\omega^n \frac{\partial \dot{\xi}_\omega}{\partial z}, \quad (57)$$

represents the linear driving/damping of the mode. It is the balance of this term with the stochastic driving that determines the amplitude of the mode.

$$(b) \times (2) \propto \delta \bar{P}_\omega^n \frac{\partial \dot{\xi}_r}{\partial z} \quad (58)$$

$$\propto \bar{P} \delta \ln \bar{P}_\omega^n \omega \Gamma_1^{-1} \delta \ln \bar{P}_r^a, \quad (59)$$

is a stochastic driving term. However, it is small in comparison to the next term, because it is proportional to the non-adiabatic coherent pressure

fluctuation which is small since the mode amplitude growth time is many periods.

$$(c) \times (1) \propto \delta \bar{P}_r^n \frac{\partial \dot{\xi}_\omega}{\partial z} \quad (60)$$

$$\propto \bar{P} \delta \ln \bar{P}_r^n \omega \Gamma_1^{-1} \delta \ln \bar{P}_\omega^a, \quad (61)$$

is the dominant stochastic driving term. It is proportional to the non-adiabatic random pressure fluctuations which are large and the adiabatic coherent pressure fluctuations which are also large, since they provide the mode restoring force.

$$(d) \times (2) \propto \delta \bar{P}_r^n \frac{\partial \dot{\xi}_r}{\partial z}, \quad (62)$$

does not represent any work on the mode (it does not contain any factor representing the mode).

### 3.2. Stochastic excitation

Using the results from the previous subsection, we may derive expressions that measure the stochastic excitation and the linear damping in numerical simulations. After proper scaling, such measurements yield estimates of global excitation power and damping that may be compared directly with estimates from observations Roca Cortes et al. (1999), and with estimates from analytical theories (e.g., Balmforth 1992b; Goldreich et al. 1994).

The mode energy per unit surface area (at  $r = R$ ) is

$$E_\omega = \frac{1}{2} \omega^2 \int_r dr \xi_\omega^2 \rho \left( \frac{r}{R} \right)^2 \equiv M_\omega V_\omega^2 \quad (63)$$

where  $M_\omega$  is (by definition) the mode mass, and  $V_\omega = \dot{\xi}_\omega(R)$  is the mode velocity amplitude at the reference radius  $R$ . The change in a mode's kinetic energy over a time interval  $\Delta t$  is

$$\begin{aligned} \Delta E_\omega &= \int_{\Delta t} dt \int_r dr \delta \bar{P} \frac{\partial \dot{\xi}_\omega}{\partial r} \\ &\equiv \int_{\Delta t} dt E_\omega^{\frac{1}{2}} W_\omega(t) \\ &\equiv E_\omega^{\frac{1}{2}} C(\omega, \Delta t), \end{aligned} \quad (64)$$

where

$$W_\omega(t) \equiv E_\omega^{-\frac{1}{2}} \int_r dr \delta \bar{P} \frac{\partial \dot{\xi}_\omega}{\partial r}, \quad (65)$$

is the instantaneous work integral for the given mode's displacement, normalized with the square root of the mode's energy, and

$$C(\omega, \Delta t) = \int_{\Delta t} dt W_\omega(t) \quad (66)$$

is the work integrated over the time interval  $\Delta t$ .

For small changes of amplitude  $V_\omega \rightarrow V_\omega + \Delta V_\omega$ . Equation 63 with the definitions in Eq. 64 give,

$$\Delta V_\omega = \frac{1}{2} M_\omega^{-\frac{1}{2}} C(\omega, \Delta t). \quad (67)$$

For a particular realization of the stochastic driving, there is a complex phase factor  $e^{i\phi}$  between  $\Delta V_\omega$  and  $V_\omega$ . The ensemble average of the mode energy  $E_\omega + \Delta E_\omega$  at  $t + \Delta t$  is proportional to the ensemble average of  $|V_\omega + \Delta V_\omega|^2$  over all phases. In this averaging the linear term  $\langle V_\omega \Delta V_\omega \rangle_{\text{ens}}$  vanishes, and one obtains from the quadratic term

$$\Delta \langle |V_\omega^2| \rangle_{\text{ens}} = \langle |\Delta V_\omega|^2 \rangle_{\text{ens}} \quad (68)$$

$$= \left\langle \left| \frac{1}{2} M_\omega^{-\frac{1}{2}} C(\omega, \Delta t) \right|^2 \right\rangle_{\text{ens}}, \quad (69)$$

so that

$$\frac{\Delta \langle E_\omega \rangle_{\text{ens}}}{\Delta t} = \frac{M_\omega \Delta \langle |V_\omega^2| \rangle_{\text{ens}}}{\Delta t} \quad (70)$$

$$= \frac{1}{4 \Delta t} \langle |C(\omega, \Delta t)|^2 \rangle_{\text{ens}}. \quad (71)$$

In terms of Fourier transforms over the time interval  $\Delta t$ , the integrated work

$$\begin{aligned} E_\omega^{\frac{1}{2}} C(\omega, \Delta t) &= \Delta t \operatorname{Re} \left[ \int_r dr \delta \bar{P}_\omega^* i \omega \frac{\partial \dot{\xi}_\omega}{\partial r} \right] \\ &= \omega \Delta t \operatorname{Im} \left[ \int_r dr \delta \bar{P}_\omega^* \frac{\partial \dot{\xi}_\omega}{\partial r} \right] \\ &\equiv \omega \Delta t \operatorname{Im} [\widehat{W}_\omega] \end{aligned} \quad (72)$$

is proportional to the Fourier amplitude of the projection of the stochastic pressure fluctuations onto  $\dot{\xi}_\omega$ .

The expectation value of the square of the imaginary part is half of the power of this random function in the frequency interval  $\Delta \nu = 1/\Delta t$ , since  $\langle |\widehat{W}_\omega|^2 \rangle_{\text{ens}} = \langle |\operatorname{Re}[\widehat{W}]|^2 \rangle_{\text{ens}} + \langle |\operatorname{Im}[\widehat{W}]|^2 \rangle_{\text{ens}}$ , and the ensemble averages for the real and imaginary parts are equal for a function with randomly distributed phases, so

$$\langle |\operatorname{Im}[\widehat{W}]|^2 \rangle_{\text{ens}} = \frac{1}{2} \langle |\widehat{W}_\omega|^2 \rangle_{\text{ens}}. \quad (73)$$

From Eqs. 70, 72 and 73, we obtain

$$\begin{aligned}\frac{\Delta\langle E_\omega \rangle_{\text{ens}}}{\Delta t} &= \frac{1}{4\Delta t} \langle \left| \frac{\omega \Delta t}{E_\omega^{\frac{1}{2}}} \text{Im}[\widehat{W}_\omega] \right|^2 \rangle_{\text{ens}} \\ &= \frac{\omega^2 \Delta t}{8E_\omega} \langle |\widehat{W}_\omega|^2 \rangle_{\text{ens}} \\ &= \frac{\omega^2 \Delta t}{8E_\omega} \langle \left| \int_r dr \delta\bar{P}_\omega^* \frac{\partial\xi_\omega}{\partial r} \right|^2 \rangle_{\text{ens}} \quad (74)\end{aligned}$$

and with the definition Eq. 63 of the mode energy, the expectation value of the stochastic excitation power is

$$\frac{\Delta\langle E_\omega \rangle_{\text{ens}}}{\Delta t} = \frac{\left| \int_r dr \delta\bar{P}_\omega^* \frac{\partial\xi_\omega}{\partial r} \right|^2}{4 \Delta\nu \int_r dr |\xi_\omega|^2 \rho \left(\frac{r}{R}\right)^2}. \quad (75)$$

From Eq. 57, the damping rate is

$$\frac{1}{E_\omega} \frac{dE_\omega}{dt} = \frac{\int_r dr \delta\bar{P} \frac{\partial\xi_\omega}{\partial r}}{\frac{1}{2}\omega^2 \int_r dr |\xi_\omega|^2 \rho \left(\frac{r}{R}\right)^2}, \quad (76)$$

or, in terms of Fourier transforms,

$$\frac{1}{E_\omega} \frac{dE_\omega}{dt} = \frac{2 \int_r dr \text{Im}[\delta\bar{P}_\omega^* \frac{\partial\xi_\omega}{\partial r}]}{\omega \int_r dr |\xi_\omega|^2 \rho \left(\frac{r}{R}\right)^2}. \quad (77)$$

Equation 75 expresses the excitation power per unit surface area in terms of the power density of the stochastic pressure fluctuations,  $\delta\bar{P}_\omega$ . If these are measured in a numerical simulation covering a small ( $L \times L$ ) patch of the solar surface, the result must be properly scaled in order to estimate global excitation power. Taking the results at face value would correspond to assuming a periodic, coherent repetition of the pressure fluctuations over the entire solar surface area  $4\pi R^2$ . If the actual pressure fluctuations are instead uncorrelated over scales larger than the scale of the numerical model, the global spectral power density is smaller by a factor of  $L^2/(4\pi R^2)$ . The integrated excitation power is then obtained by multiplying Eq. 75 with the horizontal surface area of the numerical model,  $L^2$ , rather than by the total surface area,  $4\pi R^2$ . (Note that this does not imply that the scale  $L$  enters into the final result, since the expectation value of the fluctuations of the mean pressure  $\delta\bar{P}_\omega$  drops correspondingly, if the size of the numerical model is increased beyond the size over which pressure fluctuations are correlated.)

## 4. Examples

To demonstrate that the proposed formalism is useful, both from a theoretical and a practical point of view, we provide two example applications; a theoretical discussion of deviations from hydrostatic equilibrium, and a practical application to a numerical data set.

### 4.1. Deviations from hydrostatic equilibrium

The equations for the horizontal averages (either Eqs. 17–20 or the equivalent Lagrangian equations 30–32) do not assume anything about the horizontally averaged (barred) quantities, other than that they are instantaneous, horizontal averages.

Assuming now that a stationary reference state exists, with  $\langle \bar{u}_z \rangle_t = 0$ , one may ask what happens if initially the barred variables deviate from the equilibrium state. The initial state may then be taken as an initial condition for a time integration of Eqs. 30–32.

Ignoring in a first analysis the lagrangian time variation of the terms that represent the convective flux, the radiative flux, and the turbulent pressure, one has a set of equations that are directly analogous to the ordinary, one dimensional hydrodynamic equations, and admits exactly the same type of solution; the initial non-equilibrium state slumps towards the equilibrium state, overshoots, and a series of oscillations ensues. If the boundaries are closed, and there are no dissipative terms, the oscillations will continue undamped, and consist of a superposition of the eigenmodes of the system.

If the boundaries allow wave energy to escape, and / or there are other dissipative effects, the eigenmodes will be damped, and the solution will eventually settle to the equilibrium solution.

Likewise, if one considers the actual, time-dependent lagrangian response of the convective and radiative fluxes, and of the turbulent pressure, these will in general also contribute to the damping (or possibly self-excitation) of the eigenmodes of the system.

In conclusion, an initial state that is not in hydrostatic equilibrium may be thought of as a superposition of (in general damped) eigenmodes,

and such a system will typically perform damped oscillations around a stationary reference state.

All of this might be analyzed by making use of the formalism put forward here, at any chosen level of realism; one may replace the bracketed terms that are not available in closed form with theoretical estimates, or one may retain them as they are, and evaluate them from numerical simulations. In fact, we have performed numerical experiments of just this type by subjecting snap shots from 3-D simulations to large amplitude perturbations of the vertical equilibrium, in order to study in particular the damping properties of the resulting set of oscillations. Results of the analysis will be published in a forthcoming paper.

#### 4.2. Excitation rates and energy losses in a numerical experiment

As a direct test of the expression for the excitation rate, Eq. 74, we have evaluated the expression numerically, using data from a numerical experiment covering 43 hours of solar time at a resolution of  $63 \times 63 \times 63$ —additional details about this experiment are given elsewhere. The length of this run is sufficient for a direct measurement of mode line widths, and hence for a direct determination of the right hand side of the expression

$$\frac{\Delta\langle E_\omega \rangle_{\text{ens}}}{\Delta t} = \frac{E_{\text{mode}}}{\tau_{\text{mode}}}, \quad (78)$$

where the mode energy life time  $\tau_{\text{mode}}$  is related to the full width at half maximum of the mode energy spectrum  $\Delta\nu_{\text{FWHM}}$  by

$$2\pi\tau_{\text{mode}}\Delta\nu_{\text{FWHM}} = 1. \quad (79)$$

In Fig. 1 we compare estimates of the excitation power based on Eq. 75 with the actual energy loss for the three radial modes that are observed in the experiment. The energy loss of each mode was computed from Eq. 78 by fitting Lorentzians to the excess mode power above the background noise (cf. Paper II, Fig. 1), using  $E_{\text{mode}}$  and  $\tau_{\text{mode}}$  as parameters in the fit. The excitation power was evaluated from Eq. 75, with mode displacement factors  $\frac{\partial\xi_\omega}{\partial r}$ , and  $\xi_\omega$ , obtained by using Fourier transforms to project out the three modes (cf. Fig. 2). Note that the actual amplitudes of these modes do not enter into the estimate of the excitation power,

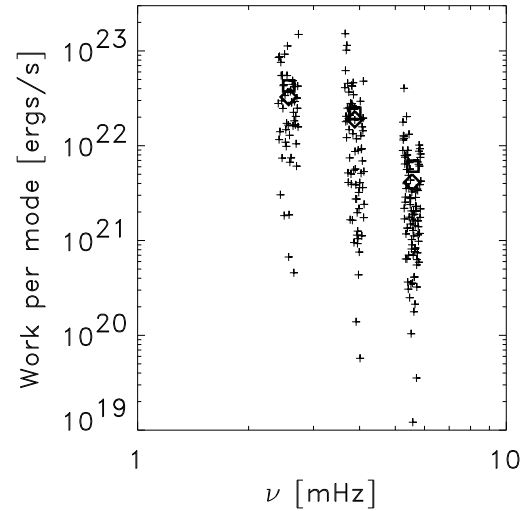


Fig. 1.— The excitation power (small pluses) in the neighborhood of the frequencies of the three radial modes that are excited to measurable amplitudes in the box. The average excitation is shown as diamonds, and the average energy loss per unit time is shown as squares. The results are from a numerical experiment with realistic opacities and equation of state, covering 43 hours of solar time at a resolution of  $63 \times 63 \times 63$  (Georgobiani et al. 2000). Note that, because of the relatively low resolution required for such a long run to be affordable, the results are not directly comparable to solar values. The mode mass of the box also differs significantly from the solar mode mass at the same frequency.

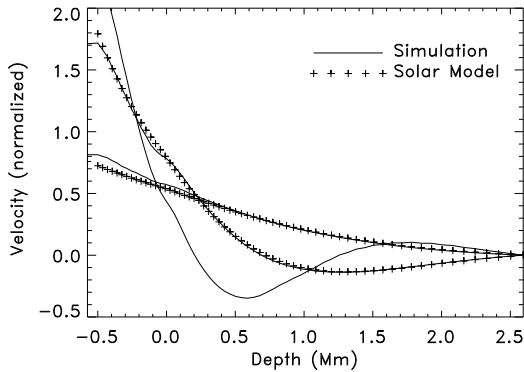


Fig. 2.— The velocity mode shapes for the three radial oscillations, at 2.5, 3.9, and 5.6 mHz, that are observed in the 43 hour simulation. For comparison, the corresponding modes from Model S of Christensen-Dalsgaard et al. (1996a), normalized to the same mode mass within the box, are also shown (plus symbols) for the two modes whose frequencies are below the acoustic cut-off frequency.

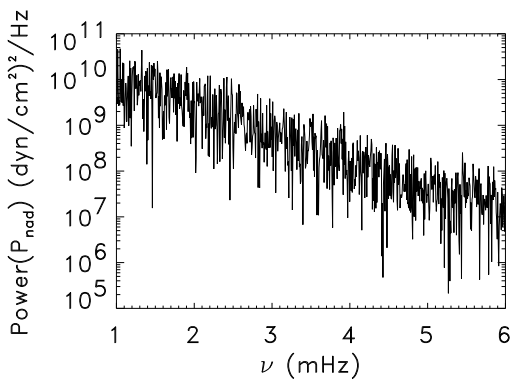


Fig. 3.— The power-spectrum of the non-adiabatic pressure fluctuations, Eq. 47, in a layer close to the surface of the 43 hour simulation.

because of the normalization with the mode kinetic energy in Eq. 75. The non-adiabatic pressure fluctuations at the mode frequencies,  $\delta\bar{P}_\omega^*$ , were obtained from the Fourier transform of the non-adiabatic pressure fluctuations (Fig. 3), averaging over a neighborhood of the mode frequencies to obtain the values indicated with diamonds in Fig. 1. For further details on how the formulae are evaluated see the appendix of Paper II.

Note that the spectrum of non-adiabatic pressure follows a power law and shows no particular features at the resonant mode frequencies. This illustrates that the non-adiabatic fluctuations are mostly incoherent. Conversely, since the modes are only weakly damped, the coherent fluctuations at the mode frequencies are mostly adiabatic. At non-mode frequencies, the fluctuations are a mix of adiabatic and non-adiabatic, incoherent fluctuations (of which only the non-adiabatic ones contribute stochastic work).

## 5. Concluding remarks

We have shown how to decompose the fluid variables into horizontal averages and fluctuations, and how to use this decomposition to separate the equations for the radial p-modes (Eqs. 30–32) from the full equations (Eqs. 9–11). The equations for the radial modes are similar to those for a 1-D stratified medium with the addition of two extra terms – the gradient of the turbulent pressure and the gradient of the convective plus kinetic energy fluxes. There are two additional subtle differences from the 1-D equations – the radiative flux may differ significantly from that of a 1-D model with the same mean structure and the gas pressure is not the same as the pressure for the average density and internal energy.

We have used the decomposed fluid equations to derive an expression for the stochastic excitation rate of the radial p-modes (Eq. 75) in terms of the  $PdV$  work of the non-adiabatic, incoherent, random, convectively produced pressure fluctuations and the mode compression, and tested the expression by applying it to a numerical experiment of sufficient length to measure the mode energy loss directly from the observed mode power and spectral line width.

The price that had to be paid for obtaining a sufficiently long duration experiment (43 solar

hours in this case) was that the numerical resolution could not be very large. From previous convergence investigations we know that various aspects of the numerical models depend to a quite varying degree on the numerical resolution (Stein & Nordlund 1998). The thermal mean structure, for example, is very robust, while the peak in relative turbulent pressure near the surface depends more sensitively on numerical resolution.

In the subsequent paper (Stein & Nordlund 2000, Paper II), we use higher resolution models to determine the mode excitation power more accurately, and compare it directly with helioseismic results. The duration of these experiments are not sufficient to allow the excited modes to be resolved in frequency, but this is not necessary to determine the mode excitation power from Eq. 75. In addition, the high resolution experiments are used to reveal the spatial locations that contribute most of the excitation power, and to investigate the nature of the mechanism responsible for the excitation.

Using the type of formalism put forward in the present paper it is also possible to analyze the mode physics (intrinsic) contributions to mode damping and frequency shifts, but this is work for the future.

The work of ÅN was supported in part by the Danish Research Foundation, through its establishment of the Theoretical Astrophysics Center. The work of RFS was supported in part by grants NAG 5-4031 and NAG 5-8053 from NASA and AST 9521785 and AST 9819799 from the US National Science Foundation. We thank the High Altitude Observatory / National Center for Atmospheric Research for hospitality during the writing of this paper.

## REFERENCES

Antia, H. M. & Chitre, S. M., eds. 1996, Bull. of the Atronomical Soc. of India, Vol. 24, Windows on the Sun's Interior

Atroshchenko, I. N. & Gadun, A. S. 1994, A&A, 291, 635

Balmforth, N. J. 1992a, 255, 632

—. 1992b, 255, 639

Bogdan, T. J., Cattaneo, F., & Malagoli, A. 1993, ApJ, 407, 316

Brown, T. M., ed. 1993, Astronomical Society of the Pacific Conference Series, Vol. 42, GONG'92: Seismic investigation of the Sun and stars, San Francisco

Christensen-Dalsgaard, J. 1988, in ESA, Seismology of the Sun and Sun-Like Stars p 431-450 (SEE N89-25819 19-92), 431-450

Christensen-Dalsgaard, J., Däppen, W., Ajukov, S. V., Anderson, E. R., Antia, H. M., Basu, S., Baturin, V. A., Berthomieu, G., Chaboyer, B., Chitre, S. M., Cox, A. N., Demarque, P., Donatowicz, J., Dziembowski, W. A., Gabriel, M., Gough, D. O., Guenther, D. B., Guzik, J. A., Harvey, J. W., Hill, F., Houdek, G., Iglesias, C. A., Kosovichev, A. G., Leibacher, J. W., Morel, P., Proffitt, C. R., Provost, J., Reiter, J., Jr., R., J., E., Rogers, F. J., Roxburgh, I. W., Thompson, M. J., & Ulrich, R. K. 1996a, Science, 272, 1286

Christensen-Dalsgaard, J., Däppen, W., & et al. 1996b, Science, 272, 1286

Christensen-Dalsgaard, J., Dappen, W., & Lebreton, Y. 1988, Nature, 336, 634

Georgobiani, D. G., Kosovichev, A. G., Nigam, R., Nordlund, Å., & Stein, R. F. 2000, ApJ, 530, L139

Goldreich, P. & Keeley, D. A. 1977, ApJ, 212, 243

Goldreich, P. & Kumar, P. 1988, ApJ, 326, 462

—. 1990, ApJ, 363, 694

Goldreich, P., Murray, N., & Kumar, P. 1994, ApJ, 424, 466

Hoeksema, J. T., Domingo, V., Fleck, B., & Battbrick, B., eds. 1995, ESA SP, Vol. 376, Fourth SOHO Workshop: Helioseismology, ESTEC,Nordwijk

Mihalas, D., Hummer, D. G., Mihalas, B. W., & Däppen, W. 1990, ApJ, 350, 300

Musielak, Z. E., Rosner, R., Stein, R. F., & Ulmschneider, P. 1994, ApJ, 423, 474

Nordlund, Å. 1982, A&A, 107, 1

—. 1985, *Solar Physics*, 100, 209

Nordlund, Å. & Dravins, D. 1990, *A&A*, 228, 155

Nordlund, Å. & Stein, R. F. 1991a, in *Stellar Atmospheres: Beyond Classical Models*, ed. L. Crivellari, I. Hubeny, & D. G. Hummer (Kluwer)

Nordlund, Å. & Stein, R. F. 1991b, in *Lecture Notes in Physics*, Vol. 388, *Challenges to Theories of the Structure of Moderate Mass Stars*, ed. D. Gough & J. Toomre (Springer, Heidelberg), 141–146

Pijpers, F. P., J. Christensen-Dalsgaard, & Rosenthal, C. S., eds. 1997, *Solar Convection, Oscillations and their Relationship; SCORe'96* (Dordrecht: Kluwer Academic Press)

Roca Cortes, T., Montanes, P., Palle, P. L., Perez Hernandez, F., Jimenez, A., Regula, C., & the GOLF Team. 1999, in *ASP Conf. Ser.*, Vol. 173, *Theory and Tests of Convective Energy Transport*, ed. A. Gimenez, E. Guinan, & B. Montesinos, 305

Rogers, F. J., Swenson, F. J., & Iglesias, C. A. 1996, *ApJ*, 456, 902

Rosenthal, C. S., Christensen-Dalsgaard, J., Kosovichev, A. G., Nordlund, A. A., Reiter, J., Rhodes, E. J., J., Schou, J., Stein, R. F., & Trampedach, R. 1998, in *Structure and Dynamics of the Interior of the Sun and Sun-like Stars, SOHO 6/GONG 98 Workshop*, E123–+

Rosenthal, C. S., Christensen-Dalsgaard, J., Nordlund, Å., Stein, R. F., & Trampedach, R. 1999, *A&A*, 351, 689

Solanki, S., Rüedi, I., Bianda, M., & Steffen, M. 1996, *A&A*, 308, 623

Steffen, M. 1988, in *Advances in Helio- and Asteroseismology*, ed. J. Christensen-Dalsgaard & S. Frandsen (Reidel, Dordrecht), 379–382

Steffen, M. & Freytag, B. 1991, in *Reviews in Modern Astronomy*, ed. G. Klare, Vol. 4 (Springer, Heidelberg), 43–60

Steffen, M., Ludwig, H.-G., & Krüss, A. 1989, *A&A*, 213, 371

Stein, R. F. 1967, *Solar Physics*, 2, 385

—. 1968, *ApJ*, 297, 154

Stein, R. F., Nordlund, Å., Kuhn, J. 1989, in *Solar and Stellar Granulation*, ed. R. Rutten & G. Severino (Kluwer Academic Press), 381–399

Stein, R. F. & Nordlund, Å. 1989, *ApJ*, 342, L95

Stein, R. F. & Nordlund, Å. 1991, in *Lecture Notes in Physics*, Vol. 388, *Challenges to Theories of the Structure of Moderate Mass Stars*, ed. D. Gough & J. Toomre (Springer, Heidelberg), 195–212

Stein, R. F. & Nordlund, Å. 1994, in *Infrared Solar Physics*, IAU Symposium 154, ed. D. Rabin, J. Jefferies, & C. Lindsey (Dordrecht: Kluwer), 225–238

—. 1998, *ApJ*, 499, 914

—. 2000, *ApJ*, (submitted)

Stein, R. F., Nordlund, Å., & Kuhn, J. R. 1988, in *ESA*, Vol. SP-286, *Proc. Symp. Seismology of the Sun and Sun-like Stars*, ed. E. J. Rolfe, 529

Ulrich, R. K., Rhodes Jr, E. J., & Däppen, W., eds. 1995, *Astronomical Society of the Pacific Conference Series*, Vol. 76, *GONG'94: Helio- and Asteroseismology from Earth and Space*, San Francisco

## Figure Captions

Fig. 1.— The excitation power (small pluses) in the neighborhood of the frequencies of the three radial modes that are excited to measurable amplitudes in the box. The average excitation is shown as diamonds, and the average energy loss per unit time is shown as squares. The results are from a numerical experiment with realistic opacities and equation of state, covering 43 hours of solar time at a resolution of  $63 \times 63 \times 63$  (Georgobiani et al. 2000). Note that, because of the relatively low resolution required for such a long run to be affordable, the results are not directly comparable to solar values. The mode mass of the box also differs significantly from the solar mode mass at the same frequency.

Fig. 2.— The velocity mode shapes for the three radial oscillations, at 2.5, 3.9, and 5.6 mHz, that are observed in the 43 hour simulation. For comparison, the corresponding modes from Model S of Christensen-Dalsgaard et al. (1996a), normalized to the same mode mass within the box, are also shown (plus symbols) for the two modes whose frequencies are below the acoustic cut-off frequency.

Fig. 3.— The power-spectrum of the non-adiabatic pressure fluctuations, Eq. 47, in a layer close to the surface of the 43 hour simulation.